Holomycin, an antibiotic secondary metabolite, is required for biofilm formation of the native producer Photobacterium galatheae S2753

Zhang, Sheng-Da; Isbrandt, Thomas; Lindqvist, Laura Louise; Larsen, Thomas Ostenfeld; Gram, Lone

Published in:
Applied and Environmental Microbiology

Link to article, DOI:
10.1128/AEM.00169-21

Publication date:
2021

Document Version
Peer reviewed version

Holomycin, an antibiotic secondary metabolite, is required for biofilm formation of the native producer *Photobacterium galatheae* S2753

Sheng-Da Zhang, Thomas Isbrandt, Laura Louise Lindqvist, Thomas Ostenfeld Larsen and Lone Gram

Department of Biotechnology and Biomedicine, Technical University of Denmark, Søltofts Plads bldg. 221, DK-2800 Kgs Lyngby, Denmark

Corresponding author: Sheng-Da Zhang, shez@dtu.dk

Running title: Role of holomycin in the native producer

Keywords: *Photobacterium galatheae,* holomycin, biosynthetic gene cluster, biofilm, secondary metabolites.

Abstract

Whilst the effects of antibiotics on microorganisms are widely studied, it remains less well-understood how antibiotics affect the physiology of the native producing organisms. Here, using a marine bacterium *Photobacterium galatheae* S2753 that produces the antibiotic holomycin, we generated a holomycin deficient strain by in-frame deletion of *hlmE*, the core gene responsible for holomycin production. Mass spectrometry analysis of cell extracts confirmed that Δ*hlmE* did not produce holomycin and that the mutant was devoid of antibacterial activity. Biofilm formation of Δ*hlmE* was significantly reduced compared to that of the wild-type S2753 and was restored in an *hlmE* complementary mutant. Consistently, exogenous holomycin, but not its dimethylated and less antibacterial derivative, S,S'-dimethyl holomycin, restored the biofilm formation of Δ*hlmE*. Furthermore, zinc starvation was found essential for both holomycin production and biofilm formation of S2753, although the molecular mechanism remains elusive. Collectively, these data suggest that holomycin promotes biofilm formation of S2753 via its ene-disulfide group. Lastly, the addition of holomycin in sub-inhibitory concentrations also enhanced the biofilm of four other Vibrionaceae strains. *P. galatheae* likely gains an ecological advantage from producing holomycin as both an antibiotic and a biofilm stimulator, which facilitates the nutrition acquisition and protects *P. galatheae* from environmental stresses. Studying the function of antibiotic compounds in the native producer will shed light on their role in nature and could potentially point to novel bioprospecting strategies.

Importance

Despite the societal impact of antibiotics, their ecological functions remain elusive and have mostly been studied by exposing non-producing bacteria to sub-inhibitory concentrations. Here, we studied the effects of the antibiotic holomycin on its native producer, *Photobacterium galatheae* S2753, a Vibrionaceae bacterium. Holomycin provides a distinct advantage to S2753 both as an antibiotic and by enhancing biofilm formation in the producer. Vibrionaceae species successfully thrive in global marine ecosystems, where they play critical ecological roles as free-living, symbiotic, or pathogenic bacteria. Genome mining has demonstrated that many have the potential to produce several bioactive compounds, including *P. galaltheae*. To unravel the contribution of the microbial metabolites to the development of marine microbial ecosystems, better insight into the function of these compounds in the producing organisms is needed. Our finding provides a model to pursue this and highlights the ecological importance of antibiotics to the fitness of the producing organisms.

Introduction

Many microbial secondary metabolites have antibiotic activity and are crucial for treating bacterial infections in modern society. The clinical doses of antibiotics deployed are often much higher than the concentrations found in the natural environments where the compounds can be difficult to detect (1, 2). This has raised the question of the natural roles of microbial antibiotics in Nature (2–9).

In Nature, bacteria live in a multispecies community, whose composition and spatial structure change dynamically in response to external nutritional and physiochemical parameters, and also as a function of inter-species interactions often mediated by bioactive molecules (2, 9, 10). Biofilms are structures associated with surfaces and the dominant bacterial lifestyles in natural environments, as it is an efficient means of persistence (11). Several bioactive secondary metabolites affect bacterial biofilm formation. For example, sub-inhibitory concentrations of tobramycin, an aminoglycoside antibiotic, induced biofilm formation of *Escherichia coli* and *Pseudomonas aeruginosa* (2, 12). Tobramycin activates an inner membrane phosphodiesterase Arr of *P. aerugenosa* PAO1, and promotes the biofilm formation likely by regulating the localized cytoplasmic c-di-GMP pools (12, 13). Both polyamine norspermine and glycine betaine, two compounds that may be produced by native marine organisms, enhance the cell density in *Vibrio cholera*e biofilms (14, 15). These studies have particularly emphasized the role of exogenous secondary metabolites in bacterial biofilm development; however, whether endogenous antibiotic compounds exert the same function is yet to be investigated.

We and others have reported that marine bacteria in the genera *Phaeobacter, Ruegeria Pseudoalteromonas,* and *Vibrionaceae* are potent producers of secondary metabolites with antibiotic activity (16–24) However, whether these compounds play other roles than being antibiotics in the microbial community is not known. Unraveling the possible roles of compounds with antibiotic activities in complex systems is challenging and we therefore chose to start our investigations in a controllable system, addressing if a compound with antibiotic activity plays any role on the physiology of the producing organism. *Photobacterium galatheae* S2753, an organism from the *Vibrionaceae* family was isolated from the surface of a green mussel (25). The bacterium produces holomycin (24), a dithiolopyrrolone (DTP) family natural product (26–29) that inhibits cell growth of tumor cells as well as a broad spectrum of organisms, e.g., yeast, Gram-negative and Gram-positive bacteria, including methicillin-resistant *Staphylococcus aureus* (MRSA) (23, 24, 28, 30). The holomycin biosynthetic pathway has been studied in *Streptomyces clavuligerus* (31) and *Yersinia ruckeri* (32), respectively. As predicted by antiSMASH (33), *P. galatheae* S2753 harbors eleven potential biosynthetic gene clusters (BGCs) with one predicted to produce holomycin (17, 23, 34). The purpose of this study, using *P. galatheae* S2753 as a model organism, was to confirm experimentally the bioinformatically predicted holomycin BGC and to determine possible role(s) of the antibiotic holomycin in the physiology and ecology of the producer. Such studies could lead to new insight into the function and ecological role(s) of secondary metabolites with antibiotic activity and potential facilitate new bioprospecting strategies.

Results

Analysis of the biosynthetic gene cluster of holomycin of *P. galatheae* S2753.

AntiSMASH version 5.0 identified eleven BGCs in *P. galatheae* S2753, of which eight were on the large chromosome and three on the small one. Based on a previous prediction (17), BGC11 on the small chromosome potentially encodes the enzymes involved in the biosynthesis of holomycin. Sequence analysis and functional annotation showed that BGC11 contains ten genes, eight of which are homologous to those in the holomycin BGCs of *Y. ruckeri* and *S. clavuligerus* (Figure 1A). Therefore, the holomycin biosynthesis in *P. galatheae* likely follows the same paths as those in *S. clavuligerus* and *Y. ruckeri* (31, 32). As a core protein, the NRPS HlmE contains a characteristic arrangement of cyclization (Cy), adenylation (A), and thiolation (T) domains (Figure 1A and Table 1). According to the proposed mechanism (31, 32), HlmE initiates the synthesis pathway by covalently loading an L-cysteine and forming a dipeptide bond with a second L-cysteine. An acyl-CoA dehydrogenase HlmB then oxidizes the thiol group to allow the cyclization of the aminopyrrolinone ring of holomycin. Subsequently, a thioesterase HlmC, a PPC-DC decarboxylase HlmF, and a FMN-dependent oxidoreductase HlmD work together to generate the second thiol group, remove one molecule of carbon dioxide, and then form a dihydroholothin molecule. At last, a N-acyltransferase HlmA adds an acetyl group to form a holomycin.

Besides the eight conserved genes, BGC11 harbors a gene *hlmX* encoding a homolog to Hom9 of *Y. ruckeri* (Table 1) and a unique gene *hlmY* (Figure 1A), which encodes a putative metallophosphoesterase (Table 1). Both HlmX and Hom9 were predicted as putative ArsR/SmtB-family transcriptional regulators

with a C-terminal rhodanese-like domain.

The other two holomycin producing bacteria, *S. clavuligerus* and *Y. ruckeri,* use different self-protection strategies during holomycin production. *S. clavuligerus* encodes a disulfide-forming dithiol oxidase HlmI to control the formation of the intramolecular disulfide bridge in holomycin (35), whileas *Y. ruckeri* deploys a RNA methyltransferase Hom12 to modify the potential holomycin antibiotic targets (32). However, a homolog of *hlmI* (35) or *hom12* (32), was not found in S2753 BGC11 nor in other places on the genome.

BGC11 is responsible for holomycin production in S2753.

To experimentally test if BGC11 indeed is responsible for holomycin production, an in-frame scarless deletion mutant of the core gene *hlmE* was generated by using homologous recombination and SacB mediated counter-selection (see details in Material and Methods). Diagnostic PCRs were performed and confirmed that *hlmE* was deleted from S2753 (Figure 1B). WT S2753 and the Δ*hlmE* strains were then grown to stationary phase in different media, i.e., the marine enriched APY medium and a marine minimal medium supplemented with chitin, glucose or mannose. The produced secondary metabolites were extracted and analyzed by high-performance liquid chromatography coupled to diode array detection and high-resolution mass spectrometry (HPLC-DAD-HRMS). Whilst holomycin was detected in WT cultures, it was not produced by the Δ*hlmE* mutant (Figure 1C, D), demonstrating that *hlmE* and thus BGC11 are responsible for the biosynthesis of holomycin in *P. galatheae* S2753. Consistently, the extracted metabolites of Δ*hlmE* cultures failed to inhibit the growth of either the Gram-negative bacterium *Vibrio anguillarum* (Figure 1E) or

148 the Gram-positive *Staphylococcus aureus* (Figure 1F), both of which were
149 inhibited by the extracts from the WT strain. The antimicrobial activity of the
150 crude extracts was complemented by ectopically expressing an *hlmE* under its
151 native promoter on the plasmid vector pBBR1-MCS2, but not by a vector control
152 (Figure 1G).

153 **Biofilm formation is reduced in the Δ*hlmE* mutant.**

154 Deletion of *hlmE* did not affect the growth rate as the doubling time during
155 exponential growth and the maximum yield were 0.71±0.04 h and 6.21±0.56 OD
156 for WT, and 0.70±0.03 h and 6.21±0.34 OD for Δ*hlmE* mutant in marine media.
157 Statistically, the growth of Δ*hlmE* was not significantly different from that of WT
158 ($p>0.05$ by student's t-test). Despite the similar growth dynamics, the Δ*hlmE*
159 mutant formed less biofilm after a two-day incubation as compared to the WT
160 (Figure 2). The biofilm formation was partially restored in the complemented
161 strain Δ*hlmE*::pBBR1-MCS2-*hlmE* that was used in Figure 1G, whereas not
162 restored in the control strain Δ*hlmE*::pBBR1-MCS2 with the empty vector (Figure
163 2). The partial complementation may be due to the varied expression time and
164 level of *hlmE.*

165 **Biofilm formation of *P. galahtheae* Δ*hlmE* is restored by exogenously applied**
166 **holomycin but not by S, S'-dimethyl–red-holomycin.**

167 Since holomycin is secreted extracellularly, the effect of holomycin production on
168 biofilm formation could be mediated by its role in inter-cellular interaction and
169 addition of exogenous holomycin should, thus, restore biofilm formation of
170 Δ*hlmE* mutant. To test this hypothesis, the production of endogenous holomycin
171 was first determined as 3.59 ± 0.05 μM in the WT biofilm formation cultures.

172 Holomycin with final concentrations of 0, 0.9, 1.8, 3.6 and 7.2 μM were then
173 added to the Δ*hlmE* cultures after 17 hours incubation at 25 °C, at the time when
174 cells entered the exponential-stationary transition phase and were expected to
175 produce holomycin . Holomycin supplied in concentrations higher than 1.8 μM
176 restored the biofilm formation of Δ*hlmE* mutant to the same level of WT cultures
177 (Figure 3, $p>0.05$ by student's t-test). To further explore the functional group of
178 holomycin in triggering biofilm formation, S, S'-dimethyl holomycin (Figure 3), a
179 methylated, less antibacterial chemical analogue of holomycin (36), was also
180 added to the Δ*hlmE* cultures after 17 hours incubation. Biofilm formation of
181 Δ*hlmE* cultures was not restored by S,S'-dimethyl holomycin of concentrations
182 even up to 7.2 μM (Figure 3), suggesting that the disulfide group seems essential
183 for the role of holomycin in triggering biofilm formation or that the two methyl
184 groups in S'S-dimethyl holomycin diminish the biological function of holomycin
185 in triggering the biofilm formation of *P. galatheae* S2753.

186 **The zinc ion concentration in media negatively correlates to the holomycin**
187 **production in *P. galatheae* S2753.**

188 The disulfide group of holomycin chelates zinc ions in reducing environments
189 (37). To test if zinc was involved in holomycin production and biofilm formation,
190 wild type *P. galatheae* was grown in mannose marine minimal medium with and
191 without zinc addition. A calibration curve of holomycin was constructed and
192 used for the quantitative analysis of holomycin production in cultures. The
193 growth of *P. galathea* was not influenced by zinc in the tested concentration;
194 however, the increasing zinc concentration gradually inhibited holomycin
195 production in WT (Figure 4). Holomycin production in WT cultures was almost

196 abolished when zinc was added up to 2 mM in the wild type cultures. Meanwhile,
197 biofilm formation of wild type *P. galatheae* was also gradually inhibited by
198 increasing zinc concentration (Figure 4). To sum up, zinc negatively influenced
199 biofilm formation and holomycin production in *P. galatheae.*

200 **Exogenous holomycin triggers biofilm formation of other marine isolates.**

201 To test whether holomycin at sub-inhibitory concentrations would affect the
202 biofilm formation of other marine bacteria, sixteen isolates from six genera (i.e.
203 *Phaeobacter, Ruegeria, Vibrio, Photobacterium, Pseudoalteromonas* and *Cobetia*)
204 from the Galathea Collection (Table 2 and 3) were grown in marine broth. We
205 first determined the minimal inhibition concentrations (MIC) of holomycin for
206 these strains. Five strains were resistant to holomycin (MIC> 93 μM, Table 2)
207 including S2754 and S2755 which were isolated from the same stone where the
208 S2753-bearing mussel was located. The MICs of other bacteria were in the
209 range 2.9-93 μM (Table 2). Holomycin was then added at sub-inhibitory
210 concentrations to the cultures at either 0 h or 17 h time point (Figure 5 and 6).
211 Biofilm formation of three *Vibrio* strains and one *Photobacterium* strain was
212 significantly enhanced by holomycin added after 17-h incubation (Figure 6),
213 while the effect was not significant when added at 0 h time point (Figure 6).
214 Biofilm formation of the other strains was not affected by holomycin at either
215 time point (Figure 5). These data showed that holomycin produced by S2753
216 could affect the biofilm formation of other marine bacterial species.

217 ## Discussion

218 Species of the Vibrionaceae family play important roles in the marine
219 environment as symbiotic, pathogenic or free-living organisms and they also

harbor a large genetic potential for production of bioactive compounds (16, 17, 24, 38–41). Genetic approaches are needed to explore these bioactive compounds and to link chemical compounds to their related biosynthetic pathways enabling understanding of the physiological and ecological roles of their secondary metabolites. In this study, using the mussel-associated bacterium *P. galatheae* S2753 as a holomycin-producing model organism, we developed a protocol (Material and Methods) to genetically manipulate S2753 and generated a holomycin deficient mutant strain, Δ*hlmE*. This confirmed that a gene likely part of a BGC (the BGC11) in S2753 is responsible for holomycin production.

Exogenously supplied antibiotics in sub-lethal concentrations can affect microbial growth and metabolism by altering gene expression, nutrient utilization, and biofilm formation (42, 43). In these studies, antibiotics were added to the culture media and expected to be perceived by bacterial signal transduction pathways leading to changes in gene expression and subsequently altered phenotypes, such as biofilm formation. Consistently, we found that when applied at the late growth stage, holomycin induced biofilm formation of other holomycin non-producing bacteria (Figure 6). However, the stimulatory effect of holomycin on S2753 might differ from these since *P. galatheae* S2753 is a native producer of holomycin. Holomycin production is tightly coupled with biofilm formation in S2753. Several lines of evidence support this: 1) the Δ*hlmE* strain is defective in both holomycin production and biofilm formation, while a genetically complemented strain of Δ*hlmE* restored holomycin production and partial biofilm formation (Figure 2). 2) Exogenously added holomycin also restored the biofilm formation of the Δ*hlmE* strain to the level of WT S2753 (Figure 3). 3)

244 When an external factor, such as high concentration of zinc was added, this led to
245 a gradual reduction of holomycin production and a parallel reduction in biofilm
246 formation (Figure 4). Holomycin, once produced, may stimulate the biofilm
247 formation of S2753 either in a direct or indirect manner. Directly, holomycin may
248 bind to and activate transcriptional regulator(s) to upregulate the expression of
249 genes involved in biofilm formation. For example, the antibiotic, bacillomycin D,
250 promotes biofilm formation of the native producing bacterium *Bacillus velezensis*
251 by binding to a transcription activator, Btr (44). The complex upregulates the
252 iron up-taking ABC transporter FeuABC and consequently increases intracellular
253 iron concentration, which cues the biofilm formation of *B. velezensis*. Indirectly,
254 holomycin may chelate metal ions (including zinc) inside the cell (37), which
255 triggers global metabolic changes and various stress response pathways, and
256 often leads to the stimulation of biofilm formation. This suggested mechanism is
257 consistent with the most prevalent hypotheses that the biofilm stimulatory
258 activity of antibiotics could be coupled to the mechanism of their toxic activity,
259 which leads to generic stress responses or other physiological changes by
260 non-lethal damage on the non-producing strains (45, 46). In line with this, the
261 analog of holomycin, S, S'-dimethyl holomycin, which is not as antibacterial as
262 holomycin, cannot form the dithiol bonds at e.g. the intracellular conditions and
263 therefore chelate metal ions, and was unable to complement the biofilm
264 formation of the Δ*hlmE* strain (Figure 3).

265 Zinc influenced both holomycin production and in biofilm formation (Figure 4)
266 as has been observed in other bacteria, as free zinc used at non bactericidal
267 concentrations inhibits biofilm formation of several pathogenic bacteria,

268 including *E.coli, S. aureus, Streptococcus suis, Actinobacillus pleuropneumoniae,*
269 *Salmonella Typhymurium,* and *Heamophilus parasuis* (74, 75). The influence of
270 zinc on biofilm formation could be via its inhibitory effect on holomycin
271 production. The reduced holomycin is believed to function as a zinc chelator
272 (zincophore), to scavenge zinc from the zinc-depended enzymes (37), similar to
273 the function of siderophores for iron scavenging. We found that the predicted
274 transcriptional regulator HlmX contains potential zinc-binding sites (Table 1),
275 which may accept free zinc ions and change its ability to bind DNA and
276 reprogram gene expression. Therefore, a non-exclusive possibility for the
277 inhibitory effect of zinc is that the availability of free zinc eliminates the need for
278 holomycin production in *P. galatheae* and that the decreased holomycin
279 production reduces biofilm formation. It is also possible that a zinc responsive
280 transcriptional regulator binds to zinc ions and thereby downregulates the
281 expression of synthases involved in holomycin production, thus influencing the
282 holomycin production and biofilm formation.

283 Antibiotics are proposed to act as weapons that provide competitive advantages
284 to the native producers in environmental niches (47). This hypothesis, indeed,
285 has been evidenced by the observations that the production of antibiotic
286 secondary metabolites, including holomycin, was significantly induced by
287 stressed conditions such as exposure to antibiotics or bacterial competitors in
288 the culturing systems (48, 49). However, antibiotic secondary metabolites may
289 play multifaceted roles in natural environments - at high concentration acting as
290 antibiotics mediating antagonism between bacterial warfare, while at low
291 concentration acting as signaling molecules involved in inter- or intracellular

292 processes (50, 51). Here and in the previous study, the production of holomycin
293 in *P. galatheae* was influenced by access to nutrient sources such as chitin (52)
294 and free-zinc ions (Figure 4), leading to the question of whether holomycin
295 serves several roles in the native producer, *P. galatheae.* Chitin is the most
296 abundant polysaccharide in marine environments and several species of the
297 Vibrionaceae family (including *P. galatheae*) form biofilm in response to chitin
298 (77). *P. galatheae* is able to catabolize chitin as a nutrition source and holomycin
299 production increased significantly in chitin-supplemented media as compared to
300 glucose media (78). Given the close coupling of holomycin production to biofilm
301 formation as revealed in this article, it is possible that chitin induces holomycin
302 production, and thereby biofilm formation, which facilitates the colonization of a
303 nutrition source. *P. galatheae* S2753 was isolated from the surface of a green
304 mussel (16, 25), which may impose a zinc starvation condition to S2753 as part
305 of its nutritional immunity system (53).

306 Altogether, we propose a preliminary model of the ecological role of holomycin in
307 S2753 by incorporating the synergistic effects of chitin and zinc. When *P.*
308 *galatheae* S2753 attaches to its eukaryotic hosts, both the host chitin and the zinc
309 starvation condition (54) induce the production of holomycin, biofilm formation
310 and consequently enhanced colonization of the host and nutrition. In turn, the
311 biofilm structure protects S2753 from marine environmental changes and
312 stresses and potentially enriches zinc ions in the vicinity of S2753 cells to
313 facilitate zinc uptake by using holomycin or other means. In addition, holomycin
314 has antibacterial activity, and when applied in the early growth stage,
315 anti-biofilm activity to other marine strains (Table 2). Therefore, the coupling

316 between holomycin production and biofilm formation confers a clear advantage
317 to the ecological survival of S2753.

318

319 ## Materials and Methods

320 **Bioinformatics analyses.**

321 The genome sequences used in this study were extracted from NCBI using the
322 access numbers and uploaded to the MaGe Genoscope for holomycin BGC
323 syntenies analysis and gene annotation (55, 56). Genomes were submitted to
324 antiSMASH version 5.0 (33) for the prediction of gene clusters involved in the
325 production of holomycin. Protein domain prediction was done in InterPro
326 domains and Conserved Domain Search Service (CD Search) (57). The DNA
327 sequencing data was analyzed using BioEdit. The sequence alignment was done
328 in ClustalX.

329 **Microorganisms and growth conditions.**

330 *Escherichia coli* strains PIR1 (Invitrogen cat. C101010, Denmark) and TOP10
331 (Invitrogen cat. 404010, Denmark) were used for cloning. WM3064 of *E. coli* (58)
332 was used as the donor strain in bacterial conjugations and grown in the presence
333 of 300 µM 2,6-diaminopimelic acid (DAP). Ten µg/mL of kanamycin (Kan) or
334 chloramphenicol (Cm) was used in the *E. coli* liquid cultures and 30 µg/mL of
335 both antibiotics were used in *E. coli* agar cultures (59). Cultures of wild type and
336 mutant strains of *P. galatheae* S2753 (16, 25) were grown in marine minimal
337 medium (52) supplemented with sole carbon sources (0.2% mannose, 0.2%
338 colloidal chitin or 0.2% glucose), marine broth 2216, marine agar 2216, modified
339 enriched growth medium (APY, (56)) containing per liter: 5 g of Peptone, 3 g of

yeast extract and EMS artificial seawater. The pH was adjusted to 7.0; 12 g of agar was added per liter of APY to prepare the agar plates. Generally, colonies appeared 15 hours after plating. In the *P. galatheae* cultures, kanamycin was added at 200 μg/mL to agar plates and 150 μg/mL to liquid cultures; chloramphenicol was used at 30 μg/mL. Zinc ions was added to the media to the working concentration from a 1 M zinc chloride stock solution (pH 6.5) in water. Sixteen marine bacteria were selected to investigate the influence of holomycin in their biofilm, of which eight strains, i.e. *Vibrio* spp. (16) S0703, S1396, S1399, S2757, S3027, S3030, *Pseudoalteromonas ruthenica* S2756 (16) and *Cobitia* sp. S3029 (16), were isolated from mussel surfaces. Both *Pseudoalteromonas piscicida* S2755 (16) and *Photobacterium* sp. S2754 (16) were sampled from a stone located in the same place of S2753. Bacteria S2541 and S2545 were also included because they belong to the genus *Photobacterium* (16). Additionally, *Ruegeria* sp. S2684 (16), *Vibrio coralliilyticus* S2052 (16), *Phaeobacter piscinae* S26 (69) as well as *Pseudoalteromonas galatheae* S4498 (16) were selected as they were studied in several previous or ongoing projects. These selected marine strains were cultured on marine agar (MA) plates or in marine broth (MB). All marine cultures were inoculated at 25 °C and all *E. coli* strains at 37 °C. The strains used in this study with genotype description are listed in Table 3.

DNA manipulation and plasmid construction.

The restriction enzymes and the quick ligase for DNA modification were purchased from New England Biolabs (NEB, Bionordika, Denmark). DNA polymerase (Takara Biomedical Technology Europe (France) and Q5 High-Fidelity Polymerase (NEB) was used for PCR amplification, except for

364 colony PCRs, which were performed using TEMPase (Ampliqon, VWR, Denmark).
365 All PCR products and plasmids were purified using GFX™ PCR DNA and Gel Band
366 Purification Kit (GE Healthcare 28-9034-70, GE) and Monarch® Plasmid
367 Miniprep Kit, respectively. All plasmids and primers were designed in the ApE- A
368 plasmid Editor (v2.0) (A program designed by M. Wayne Davis. Integrated DNA
369 Technologies (IDT, Belgium) synthesized all the primers in this study. All
370 plasmids and primers used in the study are listed in Table 4 and 5.

371 The suicide plasmid pDM4-del-*hlmE* was constructed by the restriction cloning
372 method. An approximately 1.0 kb upstream and downstream region flanking of
373 *hlmE* were amplified using primer pairs D*hlmE*-P1/2, D*hlmE*-P3/4, Table 5).
374 Amplified DNA fragments were ligated into the pJET1.2/blunt cloning vector
375 with the CloneJET PCR Cloning Kit (Thermo Scientific-K1231, Denmark);
376 subsequently, they were sub-cloned into the suicide vector pDM4 (60) by using
377 the XbaI and XhoI digestion sites to form pDM4-del-*hlmE*. Gene *hlmE*, as well as
378 its native promoter region, was amplified by primer pair P_{hlm}-*hlmE*/
379 *hlmE*-6xHis (Table 5) and cloned into the expression vector pBBR1-MCS2 via
380 KpnI and XbaI to generate the complementation plasmid pBBR1-MCS2-*hlmE*.
381 Correct plasmid assembly was confirmed by PCR (Table 5), restriction digestion,
382 and sequencing (Macrogen Europe, Netherlands).

383 **Bacterial conjugation.**

384 The electroporation of *E. coli* WM3064 and the conjugation experiments were
385 performed as described previously with some modification of the culture
386 condition (58, 59, 61). WM3064 cells carrying each plasmid were grown at 37 °C
387 in LB-DAP medium with antibiotics until an optical density (OD600nm) of 0.4-0.6.

As a donor, 1 mL of WM3064 culture was harvested by centrifugation (6000 g for 1 min). Cells were washed twice with LB medium and resuspended in 50 µL LB medium with DAP. It was then mixed with 500 µL of *P. galatheae* culture with OD600 between 0.4 and 0.5. The donor-recipient cell suspension was concentrated by centrifugation (6000 g for 1 min), resuspended with 20 µL APY medium with 300 µM DAP, mixed briefly by pipetting three times. All mixture was spotted onto a 0.22 µm pore size mixed cellulose esters (MCE) membrane (MF-Millipore-GSWP02500, Merck, Germany) placed on a MA 2216 plate with 300 µM DAP. The plate was incubated for 3-4 h at 37 °C or for 3-15 h at 25 °C. The conjugations were suspended in 1 mL of APY medium and incubated for 20 min at 25 °C. Each of 100 µL conjugations was plated onto antibiotics-containing APY plates. The plates were incubated at 25 °C for 16-24 hours. Following conjugation, single colonies were grown in 2 ml APY medium supplied with chloramphenicol at 25 °C with shaking overnight. Resulting antibiotics resistant strains were screened by PCR to determine the transconjugants.

Confirmation of the transconjugants and first cross event.

Genomic DNA for PCR analyses was isolated using a NucleoSpin® Tissue Kit according to the protocol (Macherey-Nagel, Fisher Scientific, Denmark). PCR primers are listed in Table 5. Primer pairs Cm-Fw/Rv, Km-Fw-Rv, Pc0/Pc4, Pc1/Pc2 were designed to amplify the replication region for detecting the plasmids in donor strains and transconjugants. The PCR reaction was: 94 °C for 30 sec followed by 30 cycles of 94 °C for 10 sec, 58 °C for 5sec, and 72 °C for 30 sec; and 72 °C for an additional 10 min. Routine DNA manipulations were carried out following standard methods as described above.

Construction of the *hlmE* in-frame deletion mutants in S2753.

The suicide plasmid for knocking out *hlmE* gene was constructed by restriction cloning and was transferred into S2753 by intergeneric conjugation described in the supplementary information. The PCR verified mutants, in which the suicide plasmid had integrated into the anticipated place in the S2753 genome, were grown at 25 °C in APY medium with shaking to an OD600nm of 0.5. The cells were then diluted and spread on a half-APY medium (500 mL/L APY medium, 500 mL/L distilled H_2O, 15 g Agar, pH 7.0) supplied with 10% (w/v, Con_{final}) sucrose (autoclaved at 100°C for 1 hr or filtered) and incubated at 16 °C for 48 hrs. All primers used in this study are listed in Table 3.

Purification of the deletion mutants.

P. galatheae S2753 swarms on agar plate when cultured below 42°C (unpublished data). Therefore, several purification steps following the second crossover event are required to get a genetically homogenous clone. Cells from the edge of a swarming colony were inoculated in 1 ml APY medium without antibiotics with shaking at 25 °C for eight hours. The cells were then diluted and transferred onto a new half-APY-10% sucrose medium plate and incubated under 16-18 °C for 48 hours. Single colonies on the new plate were transferred onto APY-agar and APY-agar containing 30μg/mL chloramphenicol plates. Colonies sensitive to chloramphenicol were collected and confirmed by PCR and DNA sequencing using the same protocol of verifying mutants with the first crossover. If the PCR result showed a mosaic genetic feature of the selected colonies, the purification step was repeated once or more.

435 **Extraction of liquid cultures for chemical analysis.**

436 Chemical extraction was prepared as described by Giubergia *et al.* (52). Cultures
437 were incubated at 25°C for 48 hours with shaking and then transferred to 50 mL
438 falcon tubes. An equal volume of ethyl acetate was added into the culture and
439 mixed by inversion. The mixture was incubated for 10 minutes with occasional
440 inversion until a clear division of layers was present. The organic phase (top
441 layer) was transferred to a glass tube. These tubes were placed in a 35°C heating
442 block and evaporated with nitrogen for until dry. Extracts were resuspended in
443 methanol (1/20 volume of the initial culture) and stored at -20°C.

444 **UHPLC-HRMS profiling of holomycin from the wild type and mutant strains.**

445 Chemical analysis was performed as described by Giubergia *et al*. (52). Ultra
446 high-performance liquid chromatography–high-resolution mass spectrometry
447 (UHPLC-HRMS) was performed on an Agilent Infinity 1290 UHPLC system
448 (Agilent Technologies, Santa Clara, CA) equipped with a diode array detector. The
449 separation was obtained on an Agilent Poroshell 120 phenyl-hexyl column (2.1
450 by 150 mm; particle size, 1.9 µm) with a linear gradient consisting of water and
451 acetonitrile, both buffered with 20 mM formic acid, starting at 10% acetonitrile
452 and increasing to 100% in 10 min, at which point the concentration was held for
453 2 min, returned to 10% acetonitrile in 0.1 min and left for 3 min (0.35 ml/min,
454 60 °C). An injection volume of 1 µl was used. MS detection was performed in the
455 positive detection mode on an Agilent 6545 quadrupole time of flight (QTOF) MS
456 equipped with an Agilent dual-jet-stream electrospray ion source with a drying
457 gas temperature of 250 °C, a gas flow of 8 liters/min, a sheath gas temperature of
458 300°C, and a flow rate of 12 liters/min. The capillary voltage was set to 4000 V

and nozzle voltage to 500 V. Mass spectra were recorded at 10, 20, and 40 eV as centroid data for m/z 75 to 1700 in MS mode and m/z 30 to 1700 in MS/MS mode, with an acquisition rate of 10 spectra/s. Lock mass solution in 70:30 methanol-water was infused into the second sprayer using an extra LC pump at a flow rate of 15 µl/min and a 1:100 splitter. The solution contained 1 µM tributylamine (Sigma-Aldrich) and 10 µM hexakis (2,2,3,3-tetrafluoropropoxy) phosphazene (Apollo Scientific Ltd., Cheshire, United Kingdom) as lock masses. The [M + H]+ ions (m/z 186.2216 and 922.0098, respectively) of both compounds were used. The secondary metabolite profile was analyzed in Agilent Qualitative Analysis B.07.00. Five series of calibration solutions of pure holomycin (H458490, Toronto Research Chemicals, Canada) was used to create the HPLC standard calibration curve of holomycin. Peak area of holomycin in the biofilm samples and zinc cultures was recorded and used to calculate the holomycin concentration in cultures.

Well-diffusion inhibition assay.

This experiment was performed with a modified protocol from Wietz *et al.* (24). *Vibrio anguillarum* 90-11-287 and *Staphylococcus aureus* 8325 were cultured at 25 °C for 24 h in MB and LB media, respectively. To test the susceptibility of the two pathogenic strains toward the extracts from *P. galatheae* S2753 cultures, the strains were homogeneously added into warm (44.5 °C) IO agar (3% Instant ocean, 0.3% Bacto casamino acids (BD-223050, Denmark) supplemented with 0.4% glucose, 1% Agar) (for *V. anguillarum*) or IO agar with 1% peptone (for *Staphylococcus aureus* 8325). The plates were solidified and dried in a flow bench. Wells with 6 mm diameter were punched with home-made tips and 45 µL of

483 culture extract was added to each well. The agar plates containing the *V.*
484 *anguillarum* 90-11-287 and *S. aureus* 8325 cultures were incubated at 25 and
485 37 °C for 48 and 24 h, respectively. The inhibition assay was then evaluated by
486 analyzing the formation of clearing zones around the well.

487 **Growth experiments.**

488 Precultures of *P. galatheae* WT and mutant were prepared by inoculating a single
489 colony into the proper liquid medium. After 24 hours of incubation at 25 °C, the
490 preculture was diluted to OD600nm of 0.01 in 30 mL medium in a 250 mL flask
491 and incubated at 25°C with 160 rpm shaking. The value of OD600nm was
492 measured in a 1-mL cuvette every 0.5 to 6 h for 72 h using a Novaspec III
493 Spectrophotometer (Amersham Biosciences) and plotted using Origin, version
494 2019 (OriginLab Corporation, Northampton, MA, USA). After the final OD600
495 measurement, culture diluted to 10^{-6} and 10^{-7} was plated on marine agar and
496 incubated overnight for colony counting

497 **Biofilm formation.**

498 A modified protocol based on the work of (62–64) was used. Precultures were
499 diluted to OD600nm of 0.01 in 1 mL MB. Border wells were filled with 100 µL
500 MilliQ water to prevent desiccation. The 96-well microtiter plate was incubated
501 in a humidity chamber with a wet paper towel in the bottom for 48 hrs at 25°C.
502 In the complementation experiments, growth kinetics were tracked and
503 holomycin or S,S-dimethyl-holomycin synthesized by method in Yannick et al (65)
504 were added to the cultures at the exponential-stationary transition phase (17 h).
505 In the biofilm assay of selected Galatheae Collection strains, holomycin were

506 added to cultures in a two-fold dilution from 93 uM to 1.5 uM, either at the initial
507 inoculation time or after 17-hour incubation. After incubation, OD600nm was
508 measured in a SpectraMax® i3 (Molecular Devices). Culture media and
509 non-adhering bacteria were removed and the wells were washed with 150 µL
510 MilliQ water and dried for 15 minutes in a flow bench. Each well was added 125
511 µL of 1% crystal violet and staining proceeded for 15 minutes. After removing
512 the crystal violet, wells were washed three times with 200 µL MilliQ water and
513 dried for another 15 min. An amount of 200 µL 96% ethanol was added to each
514 well and incubated for 30 minutes to dissolve the staining color. Thereafter, 100
515 µL of the ethanol-crystal violet mixture in each well was transferred to a new
516 microtiter plate. The crystal violet intensity was measured at OD590nm in a
517 SpectraMax® i3. Data were analyzed in Microsoft Excel. One way ANOVA test and
518 the statistical plot graphs were analyzed in Origin, version 2019 (OriginLab
519 Corporation, Northampton, MA, USA).

520

521 **Acknowledgements**

522 The research in this study has received funding from the European Union's
523 Horizon 2020 research and innovation programme under the Marie
524 Sklodowska-Curie grant agreement no. 713683 (COFUNDfellowsDTU) for SDZ.
525 Funding from the Danish National Research Foundation for the Center for
526 Microbial Secondary Metabolites (DNRF137) is acknowledged (LG, LLL and TOL)
527 as is funding from the Independent Research Fund Denmark (project
528 7017-00003B) (SDZ, TI). This is Galatheae publication number Px (x added if

accepted).

We thank Jan Martinussen, Mogens Kilstrup, Roberto Kolter, Yong E. Zhang and Demeng Tan for helpful discussions. We thank Haitao Chen and Tao Song for providing strain WM3064 and vector pBBR1-MCS2.

TABLE AND FIGURE LEGENDS

TABLE 1 Proposed function of open reading frames (ORFs) in BGC11 of *Photobacterium galatheae* S2753. Identity scores between ORFs in BGC11 and those in the reported holomycin biosynthetic gene clusters were compared at the amino acid level.

TABLE 2 Minimal inhibitory concentration (MIC) of holomycin against selected marine bacteria.

TABLE 3 Strains used in this study.

TABLE 4. Plasmids used in this study.

TABLE 5 Primers used in this study.

FIGURE 1. **(A)** Comparison of biosynthetic gene clusters of holomycin. The genes are marked with the respective numbers or letters. Genes coding for proteins with same function are highlighted in same color. Gene assigned to NRPS are marked with domains: PCP, peptidyl carrier protein; A, adenylation domain; Cy, cyclization domain. Sequentially homologous genes are linked with dot lines. **(B)**. Diagram of the wild type *hlmE* gene region and a scarless in-frame deletion of *hlmE* gene in S2753. Left: A schematic illustration for the primers used, their annealing sites and predicted PCR products in S2753 wild type (WT) and Δ*hlmE* strains, respectively. Right: Diagnostic PCRs of the *hlmE* gene region in WT and Δ*hlmE* strains. **(C, D)**. In-frame deletion of the core gene *hlmE* completely abolished the holomycin production of Δ*hlmE* strain. Base peak and extracted ion chromatograms (m/z = 214.9943) of

555 culture extracts are shown in grey and black, respectively. UV-VIS data at 390 ± 10
556 nm also showing termination of holomycin production in the deletion strain. Red
557 asterisk symbol '*' indicates the peak of holomycin in the detection. **(E, F)**.
558 Antimicrobial activity of culture extracts against the Gram-negative bacterium *Vibrio*
559 *anguillarum* 90-11-287 and the Gram-positive bacterium *Staphylococcus aureus* 8325.
560 Crude extracts of the WT cultures and culture media (blank) were used as the positive
561 and negative control, respectively. **(G)** Antimicrobial activity of culture extracts of
562 Δ*hlmE*::pBBR1-MCS2-*hlmE* (Δ*hlmE*::*hlmE*) and *Δ*hlmE*::pBBR1-MCS2 (Δ*hlmE*::NC)
563 against the Gram-negative bacterium *Vibrio anguillarum* 90-11-287. Crude extracts of
564 the WT and cultures and Δ*hlmE* were used as the positive and negative control,
565 respectively.

566 **FIGURE 2.** Boxplot of the biofilm produced by *Photobacterium galatheae* S2753
567 wildtype (WT), Δ*hlmE,* Δ*hlmE*::pBBR1-MCS2 (Δ*hlmE*::NC) and
568 Δ*hlmE*::pBBR1-MCS2-*hlmE* (Δ*hlmE*::*hlmE*) strains. Underneath each bar is the
569 crystal violet staining of the biofilm. At least eight biological replicates were
570 performed for each strain. Error bars represent the standard division.

571 **FIGURE 3.** Biofilm formation of wild type S2753 and Δ*hlmE* strains in the presence
572 of exogenously applied holomycin (**1**) or S,S'-dimethyl holomycin (**2**). At least
573 eight biological replicates were performed for each condition. Error bars represent the
574 standard division. For all panels, two-way analysis of variance (ANOVA) was used
575 for statistical analysis. ***, $P < 0.001$.

576 **FIGURE 4.** Holomycin production (black columns) and biofilm formation (white

columns) of wild type *Photobacterium galatheae* S2753 in the presence of increasing zinc in the marine minimal medium with mannose. Three and nine biological replicates were performed in detecting holomycin production and biofilm formation, respectively. Error bars represent the standard division.

FIGURE 5. Overview of the relative biofilm formation of selected marine bacteria by sub-inhibitory concentration of holomycin. The relative biofilm formation was calculated by divided by the OD590/OD600 value of cultures without added holomycin. Error bars represent the standard division of three biological replicates.

FIGURE 6. Biofilm formation of four Galatheae collection bacteria when sub-inhibitory holomycin were added to the cultures at the initial inoculation time (0 h) or after 17-h incubation at 25 ^{o}C (17 h). Crystal violet staining were used to access the biofilm formation in the 2-day incubation cultures. Error bars represent the standard division. A. *Vibrio* sp. S1396. B. *Vibrio* sp. S1399. C. *Vibrio coralliilyticus* S2052. D. *Photobacterium* sp. S2541. Three biological replicates were performed. Error bars represent the standard division.

REFERENCES

1. Andersson DI, Hughes D. 2014. Microbiological effects of sublethal levels of antibiotics. Nat Rev Microbiol 12:465–478.

2. Linares JF, Gustafsson I, Baquero F, Martinez JL. 2006. Antibiotics as intermicrobiol signaling agents instead of weapons. Proc Natl Acad Sci U S A 103:19484–19489.

3. Bérdy J. 2005. Bioactive microbial metabolites: A personal view. J Antibiot (Tokyo).

4. Romero D, Traxler MF, L Opez D, Kolter R, López D, Kolter R. 2011.

601 Antibiotics as signal molecules. Chem Rev 111:5492–5505.

602 5. Pishchany G, Kolter R. 2020. On the possible ecological roles of antimicrobials.
603 Mol Microbiol 113:580–587.

604 6. Davies J. 2006. Are antibiotics naturally antibiotics?, p. 496–499. *In* Journal of
605 Industrial Microbiology and Biotechnology.

606 7. Oliveira NM, Martinez-Garcia E, Xavier J, Durham WM, Kolter R, Kim W,
607 Foster KR. 2015. Biofilm formation as a response to ecological competition.
608 PLOS Biol 13:e1002191.

609 8. Townsley L, Shank EA. 2017. Natural-product antibiotics: cues for modulating
610 bacterial biofilm formation. Trends Microbiol. Elsevier Ltd.

611 9. Sengupta S, Chattopadhyay MK, Grossart HP. 2013. The multifaceted roles of
612 antibiotics and antibiotic resistance in nature. Front Microbiol 4:Ariticle 47.

613 10. Davies J. 1996. Origins and evolution of antibiotic resistance. Microbiologia.

614 11. Flemming HC, Wuertz S. 2019. Bacteria and archaea on Earth and their
615 abundance in biofilms. Nat Rev Microbiol 17:247–260.

616 12. Hoffman LR, D'Argenio DA, MacCoss MJ, Zhang Z, Jones RA, Miller SI.
617 2005. Aminoglycoside antibiotics induce bacterial biofilm formation. Nature
618 436:1171–1175.

619 13. Tahrioui A, Duchesne R, Bouffartigues E, Rodrigues S, Maillot O, Tortuel D,
620 Hardouin J, Taupin L, Groleau MC, Dufour A, Déziel E, Brenner-Weiss G,
621 Feuilloley M, Orange N, Lesouhaitier O, Cornelis P, Chevalier S. 2019.
622 Extracellular DNA release, quorum sensing, and PrrF1/F2 small RNAs are key
623 players in *Pseudomonas aeruginosa* tobramycin-enhanced biofilm formation.
624 npj Biofilms Microbiomes 5:1–11.

625 14. Karatan E, Duncan TR, Watnick PI. 2005. NspS, a predicted polyamine sensor,
626 mediates activation of *Vibrio cholerae* biofilm formation by norspermidine. J
627 Bacteriol 187:7434–7443.

15. Kapfhammer D, Karatan E, Pflughoeft KJ, Watnick PI. 2005. Role for glycine betaine transport in *Vibrio cholerae* osmoadaptation and biofilm formation within microbial communities. Appl Environ Microbiol 71:3840–3847.

16. Gram L, Melchiorsen J, Bruhn JB. 2010. Antibacterial activity of marine culturable bacteria collected from a global sampling of ocean surface waters and surface swabs of marine organisms. Mar Biotechnol 12:439–451.

17. Machado H, Sonnenschein EC, Melchiorsen J, Gram L. 2015. Genome mining reveals unlocked bioactive potential of marine Gram-negative bacteria. BMC Genomics 16:158.

18. Porsby CH, Webber MA, Nielsen KF, Piddock LJ V, Gram L. 2011. Resistance and tolerance to tropodithietic acid, an antimicrobial in aquaculture, is hard to select. Antimicrob Agents Chemother 55:1332–1337.

19. Sonnenschein EC, Phippen CBW, Bentzon-Tilia M, Rasmussen SA, Nielsen KF, Gram L. 2018. Phylogenetic distribution of roseobacticides in the *Roseobacter* group and their effect on microalgae. Environ Microbiol Rep 10:383–393.

20. Wang R, Gallant É, Seyedsayamdost MR. 2016. Investigation of the Genetics and Biochemistry of Roseobacticide Production in the *Roseobacter* Clade Bacterium *Phaeobacter inhibens*. MBio 7:e02118-15.

21. Paulsen SS, Strube ML, Bech PK, Gram L, Sonnenschein EC. 2019. Marine chitinolytic *Pseudoalteromonas* represents an untapped reservoir of bioactive potential. mSystems 4:1–12.

22. Vynne NG, Månsson M, Nielsen KF, Gram L. 2011. Bioactivity, chemical profiling, and 16S rRNA-based phylogeny of *Pseudoalteromonas* strains collected on a global research cruise. Mar Biotechnol 13:1062–1073.

23. Mansson M, Gram L, Larsen TO. 2011. Production of bioactive secondary metabolites by marine *Vibrionaceae*. Mar Drugs 9:1440–1468.

655 24. Wietz M, Mansson M, Gotfredsen CH, Larsen TO, Gram L. 2010. Antibacterial
656 compounds from marine *Vibrionaceae* isolated on a global expedition. Mar
657 Drugs 8:2946–2960.

658 25. Machado H, Giubergia S, Mateiu RV, Gram L. 2015. *Photobacterium*
659 *galatheae* sp. nov, a bioactive bacterium isolated from a mussel in the Solomon
660 Sea. Int J Syst Evol Microbiol 65:4503–4507.

661 26. Kenig M, Reading C. 1979. Holomycin and an antibiotic (mm 19290) related
662 to tunicamycin, metabolites of *Streptomyces clavuligerus*. J Antibiot (Tokyo)
663 32:549–554.

664 27. Liras P. 2014. Holomycin, a dithiolopyrrolone compound produced by
665 *Streptomyces clavuligerus*. Appl Microbiol Biotechnol 98:1023–1030.

666 28. Li B, Wever WJ, Walsh CT, Bowers AA. 2014. Dithiolopyrrolones:
667 biosynthesis, synthesis, and activity of a unique class of disulfide-containing
668 antibiotics. Nat Prod Rep 31:905–923.

669 29. Qin Z, Huang S, Yu Y, Deng H. 2013. Dithiolopyrrolone natural products:
670 Isolation, synthesis and biosynthesis. Mar Drugs 11:3970–3997.

671 30. Oliva B, O'Neill A, Wilson JM, O'Hanlon PJ, Chopra I. 2001. Antimicrobial
672 properties and mode of action of the pyrrothine holomycin. Antimicrob Agents
673 Chemother 45:532–539.

674 31. Li B, Walsh CT. 2010. Identification of the gene cluster for the
675 dithiolopyrrolone antibiotic holomycin in *Streptomyces clavuligerus*. Proc Natl
676 Acad Sci U S A 107:19731–5.

677 32. Qin Z, Baker AT, Raab A, Huang S, Wang T, Yu Y, Jaspars M, Secombes CJ,
678 Deng H. 2013. The fish pathogen *Yersinia ruckeri* produces holomycin and
679 uses an RNA methyltransferase for self-resistance. J Biol Chem 288:14688–
680 14697.

681 33. Blin K, Shaw S, Steinke K, Villebro R, Ziemert N, Lee SY, Medema MH,

682 Weber T. 2019. antiSMASH 5.0: updates to the secondary metabolite genome
683 mining pipeline 47:W81–W87.

684 34. Machado H, Månsson M, Gram L. 2014. Draft genome sequence of
685 *Photobacterium halotolerans* S2753, producer of bioactive secondary
686 metabolites. Genome Announc 2:e00535-14.

687 35. Li B, Walsh CT. 2011. *Streptomyces clavuligerus* HlmI is an intramolecular
688 disulfide-forming dithiol oxidase in holomycin biosynthesis. Biochemistry
689 50:4615–4622.

690 36. Li B, Forseth RR, Bowers AA, Schroeder FC, Walsh CT. 2012. A backup plan
691 for self-protection: S-methylation of holomycin biosynthetic intermediates in
692 Streptomyces clavuligerus. Chembiochem 13:2521–6.

693 37. Chan AN, Shiver AL, Wever WJ, Razvi SZA, Traxler MF, Li B. 2017. Role for
694 dithiolopyrrolones in disrupting bacterial metal homeostasis. Proc Natl Acad
695 Sci U S A 114:2717–2722.

696 38. Ziemert N, Alanjary M, Weber T. 2016. The evolution of genome mining in
697 microbes-a review. Nat Prod Rep. Royal Society of Chemistry.

698 39. Teschler JK, Zamorano-Sánchez D, Utada AS, Warner CJA, Wong GCL,
699 Linington RG, Yildiz FH. 2015. Living in the matrix: Assembly and control of
700 *Vibrio cholerae* biofilms. Nat Rev Microbiol. Nature Publishing Group.

701 40. Yildiz FH, Visick KL. *Vibrio* biofilms: so much the same yet so different.

702 41. Takemura AF, Chien DM, Polz MF. 2014. Associations and dynamics of
703 vibrionaceae in the environment, from the genus to the population level. Front
704 Microbiol. Frontiers Research Foundation.

705 42. Schlomann BH, Wiles TJ, Wall ES, Guillemin K, Parthasarathy R. 2019.
706 Sublethal antibiotics collapse gut bacterial populations by enhancing
707 aggregation and expulsion. Proc Natl Acad Sci U S A 116:21392–21400.

708 43. O'Toole GA, Stewart PS. 2005. Biofilms strike back. Nat Biotechnol. Nature

Publishing Group.

44. Xu Z, Mandic-Mulec I, Zhang H, Liu Y, Sun X, Feng H, Xun W, Zhang N, Shen Q, Zhang R. 2019. Antibiotic bacillomycin D affects iron acquisition and biofilm formation in *Bacillus velezensis* through a Btr-mediated FeuABC-dependent pathway. Cell Rep 29:1192-1202.e5.

45. Ranieri MR, Whitchurch CB, Burrows LL. 2018. Mechanisms of biofilm stimulation by subinhibitory concentrations of antimicrobials. Curr Opin Microbiol. Elsevier Ltd.

46. Kong H, Cheng W, Wei H, Yuan Y, Yang Z, Zhang X. 2019. An overview of recent progress in siderophore-antibiotic conjugates. Eur J Med Chem. Elsevier Masson SAS.

47. Cornforth DM, Foster KR. 2015. Antibiotics and the art of bacterial war. Proc Natl Acad Sci U S A.

48. Yan Q, Lopes LD, Shaffer BT, Kidarsa TA, Vining O, Philmus B, Song C, Stockwell VO, Raaijmakers JM, McPhail KL, Andreote FD, Chang JH, Loper JE. 2018. Secondary metabolism and interspecific competition affect accumulation of spontaneous mutants in the GacS-GacA regulatory system in <i>Pseudomonas protegens. MBio 9.

49. Buijs Y, Isbrandt T, Zhang S-D, Larsen TO, Gram L. 2020. The antibiotic andrimid produced by *Vibrio coralliilyticus* increases antibiotics holomycin production in the ecological neighbour, *Photobacterium galatheae*. Appl Environ Microbiol submitted.

50. Davies J, Spiegelman GB, Yim G. 2006. The world of subinhibitory antibiotic concentrations. Curr Opin Microbiol 9:445–453.

51. Davies J. 2013. Specialized microbial metabolites: Functions and origins. J Antibiot (Tokyo). Nature Publishing Group.

52. Giubergia S, Phippen C, Nielsen KF, Gram L. 2017. Growth on chitin impacts

the transcriptome and metabolite profiles of antibiotic-producing *Vibrio coralliilyticus* S2052 and *Photobacterium galatheae* S2753. mSystems 2:1–12.

53. Capdevila DA, Wang J, Giedroc DP. 2016. Bacterial strategies to maintain zinc metallostasis at the host-pathogen interface. J Biol Chem. American Society for Biochemistry and Molecular Biology Inc.

54. Grim KP, Radin JN, Solórzano PKP, Morey JR, Frye KA, Ganio K, Neville SL, McDevitt CA, Kehl-Fie TE. 2020. Intracellular accumulation of staphylopine can sensitize *Staphylococcus aureus* to host-imposed zinc starvation by chelation-independent toxicity. J Bacteriol 202:e00014-20.

55. Ji B, Zhang S-D, Arnoux P, Rouy Z, Alberto F, Philippe N, Murat D, Zhang WJ, Rioux JB, Ginet N, Sabaty M, Mangenot S, Pradel N, Tian J, Yang J, Zhang L, Zhang W, Pan H, Henrissat B, Coutinho PM, Li Y, Xiao T, Médigue C, Barbe V, Pignol D, Talla E, Wu LF. 2014. Comparative genomic analysis provides insights into the evolution and niche adaptation of marine Magnetospira sp. QH-2 strain. Environ Microbiol 16:525–544.

56. Zhang S-D, Santini CL, Zhang WJ, Barbe V, Mangenot S, Guyomar C, Garel M, Chen HT, Li XG, Yin QJ, Zhao Y, Armengaud J, Gaillard JC, Martini S, Pradel N, Vidaud C, Alberto F, Médigue C, Tamburini C, Wu LF. 2016. Genomic and physiological analysis reveals versatile metabolic capacity of deep-sea Photobacterium phosphoreum ANT-2200. Extremophiles 20:301–310.

57. Marchler-Bauer A, Bo Y, Han L, He J, Lanczycki CJ, Lu S, Chitsaz F, Derbyshire MK, Geer RC, Gonzales NR, Gwadz M, Hurwitz DI, Lu F, Marchler GH, Song JS, Thanki N, Wang Z, Yamashita RA, Zhang D, Zheng C, Geer LY, Bryant SH. 2017. CDD/SPARCLE: Functional classification of proteins via subfamily domain architectures. Nucleic Acids Res 45:D200–D203.

58. Chen H, Zhang S-D, Chen L, Cai Y, Zhang WJ, Song T, Wu LF. 2018. Efficient genome editing of Magnetospirillum magneticum AMB-1 by CRISPR-Cas9 system for analyzing magnetotactic behavior. Front Microbiol 9:1569.

765 59. Wang H, Li Z, Jia R, Hou Y, Yin J, Bian X, Li A, Müller R, Stewart AF, Fu J,
766 Zhang Y. 2016. RecET direct cloning and Redαβ recombineering of
767 biosynthetic gene clusters, large operons or single genes for heterologous
768 expression. Nat Protoc 11:1175–1190.

769 60. Milton DL, O'Toole R, Hörstedt P, Wolf-Watz H, Toole RO, Horstedt P. 1996.
770 Flagellin A is essential for the virulence of *Vibrio anguillarum*. J Bacteriol
771 178:1310–1319.

772 61. Yin QJ, Zhang WJ, Qi XQ, Zhang S Da, Jiang T, Li XG, Chen Y, Santini CL,
773 Zhou H, Chou IM, Wu LF. 2018. High hydrostatic pressure inducible
774 trimethylamine N-oxide reductase improves the pressure tolerance of
775 piezosensitive bacteria *Vibrio fluvialis*. Front Microbiol 8:2646.

776 62. Jensen A, Larsen MH, Ingmer H, Vogel BF, Gram L. 2007. Sodium chloride
777 enhances adherence and aggregation and strain variation influences
778 invasiveness of *Listeria monocytogenes* strains. J Food Prot 70:592–599.

779 63. O'Toole GA, Kolter R. 1998. Initiation of biofilm formation in *Pseudomonas*
780 *fluorescens* WCS365 proceeds via multiple, convergent signalling pathways: A
781 genetic analysis. Mol Microbiol 28:449–461.

782 64. Djordjevic D, Wiedmann M, McLandsborough LA. 2002. Microtiter plate
783 assay for assessment of *Listeria monocytogenes* biofilm formation. Appl
784 Environ Microbiol 68:2950–2958.

785 65. Buijs Y, Zhang S-D, Jørgensen KM, Isbrandt T, Larsen TO, Gram L, Buijs Y,
786 Zhang S-D, Jørgensen KM, Isbrandt T, Larsen TO, Gram L. 2021.
787 Enhancement of antibiotic production by co-cultivation of two antibiotic
788 producing marine Vibrionaceae strains. FEMS Microbiol Ecol.

789

TABLE 1 Proposed function of open reading frames (ORFs) in BGC11 of *Photobacterium galatheae* S2753. Identity scores between ORFs in BGC11 and those in the reported holomycin biosynthetic gene clusters were compared at the amino acid level.

ORFs in *P. galatheae* S2753(17)	**Homolog in *Yersinia ruckeri* (Identity %) (32)**	**Homolog in *S. clavuligerus* ATCC 27064 (Identity %) (31)**	**Proposed function**
HlmF	Hom1 (68%)	HlmF (59%)	PPC-DC decarboxylase
HlmY	/	/	Conserved protein of unknown functions with metallophosphoesterase domain.
HlmG	Hom2 (68%)	HlmG (64%)	Globin
HlmA	Hom3 (40%)	HlmA (37%)	N-acyltransferase
HlmB	Hom4 (64%)	HlmB (52%)	Acyl-CoA dehydrogenase
HlmC	Hom5 (50%)	HlmC (38%)	Thioesterase
HlmD	Hom6 (56%)	HlmD (47%)	FMN-dependent oxdioreductase
HlmE	Hom7 (51%)	HlmE (49%)	NRPS (Cy-A-T)
HlmH	Hom8 (59%)	HlmH (62%)	MFS transporter
HlmX	Hom9 (62%)	/	Transcriptional regulator, containing a N-termianl zinc iron mediated DNA binding domain and a C-terminal Rhodanese-like domain

TABLE 2 Minimal inhibitory concentration (MIC) of holomycin against selected marine bacteria.

Strains	**MIC (µM)**
Phaeobacter piscinae S26 (69)	46.5
Vibrio sp. S0703 (16)	2.9
Vibrio sp. S1396 (16)	23.3
Vibrio sp. S1399 (16)	23.3
Vibrio coralliilyticus S2052 (16)	23.3
Photobacterium sp. S2541 (16)	23.3
Photobacterium sp. S2545 (16)	2.9
Ruegeria sp. S2684 (16)	>93
Photobacterium sp. S2754 (16)	>93
Pseudoalteromonas piscicida S2755 (16)	>93
Pseudoalteromonas ruthenica S2756 (16)	93
Vibrio sp. S2757 (16)	>93
Vibrio sp. S3027 (16)	93
Cobitia sp. S3029 (16)	23.3
Vibrio sp. S3030 (16)	11.6
Pseudoalteromonas galatheae S4498 (16)	>93

TABLE 3 Strains used in this study

Strains	Genotype/Features	Reference or source
Escherichia coli		
TOP10	F⁻ *mcrA Δ(mrr-hsdRMS-mcrBC) φ80lacZΔM15 ΔlacX74 recA1 araD139 Δ(ara-leu)7697 galU galK λ– rpsL(StrR) endA1 nupG*	Invitrogen™
PIR1	F⁻ Δ*lac169 rpoS(Am) robA1 creC510 hsdR514 endA recA1 uidA(ΔMluI)::pir-116*	Invitrogen™
WM3064	*thrB1004 pro thi rpsL hsdS lacZΔM15 RP4-1360 Δ(araBAD)567 ΔdapA1341::[erm pir]*	Strain developed by William Metcalf at UIUC
BL21(DE3)	*E. coli B dcm ompT hsdS(rB-mB-) gal λDE3*	Studier and Moffatt, 1986 (67)
***Photobacterium galatheae* S2753**		
Wildtype (WT)	Wild type	Machado *et al.*, 2015 (25)
Δ*hlmE*	In-frame deletion of *hlmE gene.*	This study
Δ*hlmE::NC*	*ΔhlmE* pBBR1-MCS2	This study
Δ*hlmE::hlmE*	*ΔhlmE.* pBBR1-MCS2-*hlmE*	This study
***Phaeobacter piscinae* S26**	Isolateed from a Greek sea bass aquaculture unit	Sonnenschein *et al.,*2017 (69)
***Vibrio* sp. S0703**	Galatheae collection strain	Gram *et al.*, 2010 (16)
***Vibrio* sp. S1396**	Galatheae collection strain	Gram *et al.*, 2010 (16)
***Vibrio* sp. S1399**	Galatheae collection strain	Gram *et al.*, 2010 (16)
***Vibrio* sp. S2757**	Galatheae collection strain	Gram *et al.*, 2010 (16)
***Vibrio* sp. S3027**	Galatheae collection strain	Gram *et al.*, 2010 (16)
***Vibrio* sp. S3030**	Galatheae collection strain	Gram *et al.*, 2010 (16)
***Vibrio coralliilyticus* S2052**	Galatheae collection strain	Gram *et al.*, 2010 (16)
***Photobacterium* sp. S2541**	Galatheae collection strain	Gram *et al.*, 2010 (16)
***Photobacterium* sp. S2545**	Galatheae collection strain	Gram *et al.*, 2010 (16)
***Photobacterium* sp. S2754**	Galatheae collection strain	Gram *et al.*, 2010 (16)
***Pseudoalteromonas piscicida* S2755**	Galatheae collection strain	Gram *et al.*, 2010 (16)
***Pseudoalteromonas ruthenica* S2756**	Galatheae collection strain	Gram *et al.*, 2010 (16)
***Pseudoalteromonas galatheae* S4498**	Galatheae collection strain	Gram *et al.*, 2010 (16)
***Ruegeria* sp. S2684**	Galatheae collection strain	Gram *et al.*, 2010 (16)
***Cobitia* sp. S3029**	Galatheae collection strain	Gram *et al.*, 2010 (16)

TABLE 4 Plasmids used in this study

Plasmids	Features	Reference
pJET1.2/blunt	Origin of replication (pMB1), Amp^R, P_{lacUV5}, *eco47IR*, T7 promoter.	Thermo Scientific™
pJET1.2-del-*hlmE*	pJET1.2/blunt. recombineering arms of gene *hlmE*	This study
pDM4	Origin of replication (R6Kγ origin), *sacB*, Cm^R.	Milton *et al.*, 1996 (61)
pDM4-d-*hlmE*	pDM4. recombineering arms of gene *hlmE*	This study
pBBR1-MCS2	Origin of replication (pBBR1), Kan^R, P_{lac}, *lacZα*	Obranić *et al.*, 2013 (68)
pBBR1-MCS2-P_{hlmE}-*hlmE*	pBBR1-MCS2, P_{hlmE}, *hlmE*-6xHis	This study

TABLE 5 Primers used in this study

Primer	Sequence (5'→3')	Description
D*hlmE*-P1	GCtctagaTGGATTGATCGCCAGTGGAG (XbaI)	Amplification of the left recombineering arm of *hlmE* gene.
D*hlmE*-P2	GTTGAGGCGTACTCAAGTGGGTCATGCGTCCTTC	
D*hlmE*-P3	GACGCATGACCCACTTGAGTACGCCTCAACAAAAAGC	Amplification of right recombineering arm of *hlmE* gene.
D*hlmE*-P4	CCGctcgagAAGTCCGGAATGACAGACGC (XhoI)	
hlmE-fw	ATGAACCCTGATCACGTTGG	Amplification of *hlmE* gene.
hlmE-rv	TCACAAGCTGACTCCGTCC	
Pc0	CCTCACATCAATCCGGATTGG	Primers used for confirmation of the in-frame deletion mutant via PCR amplification and Sequencing.
Pc1	GGTCTGGCATGGTTCTTGAC	
Pc2	TTCAGCTTCGCCTGGTAATG	
Pc3	GTGTCTGAGACCGAACAACG	
Pc4	TATCTGTCAGCGGCTGTTCC	
Pc5	GCAAGCCAATCTGGACATCC	
P_{hlm}-*hlmE*	GGggtaccGGTGAAGCAGGATAAGTGTG (KpnI)	Amplification of *hlmE* for complementation plasmid cloning
***hlmE*-6xHis**	GCtctagaTCAgtgatggtgatggtgatgCAAGCTGACTCCGTCCGG (XbaI)	
Cm-fw	GGCATTTCAGTCAGTTGCTC	Amplification of the Cm^R gene in pDM4
Cm-rv	CCATCACAAACGGCATGATG	
Km-fw	CGATACCGTAAAGCACGAGG	Amplification of the Kan^R gene in pBBR1-MCS2
Km-rv	CTCGACGTTGTCACTGAAGC	

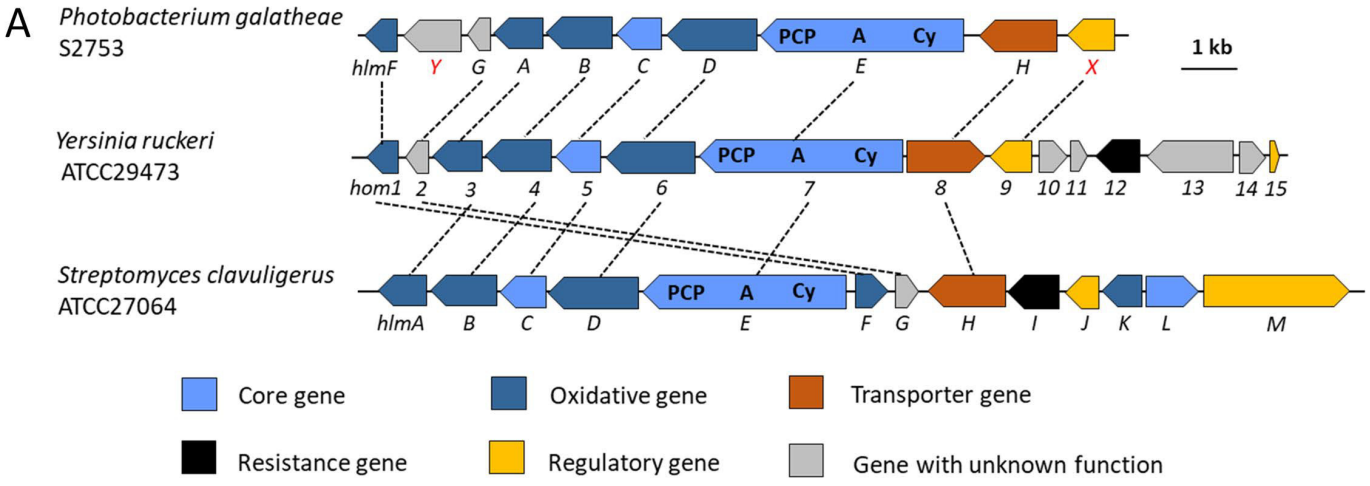

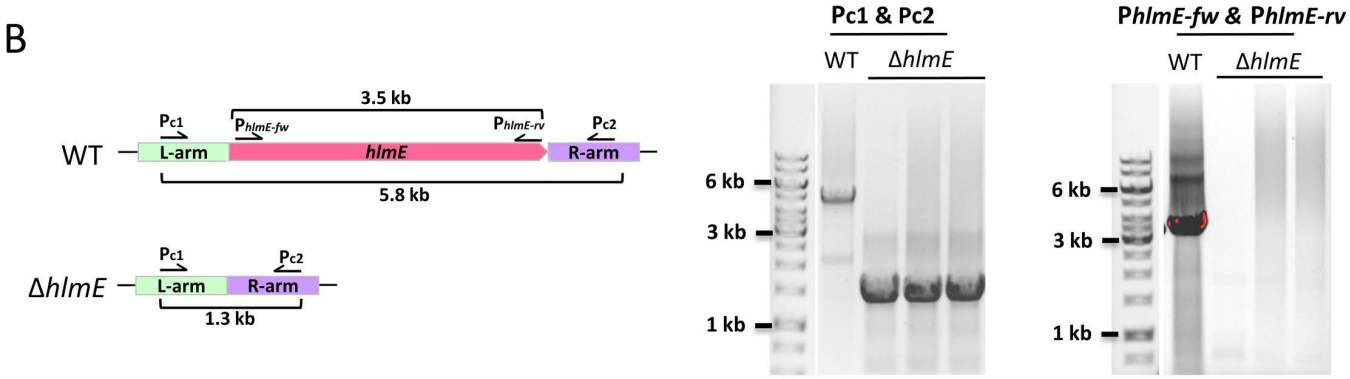

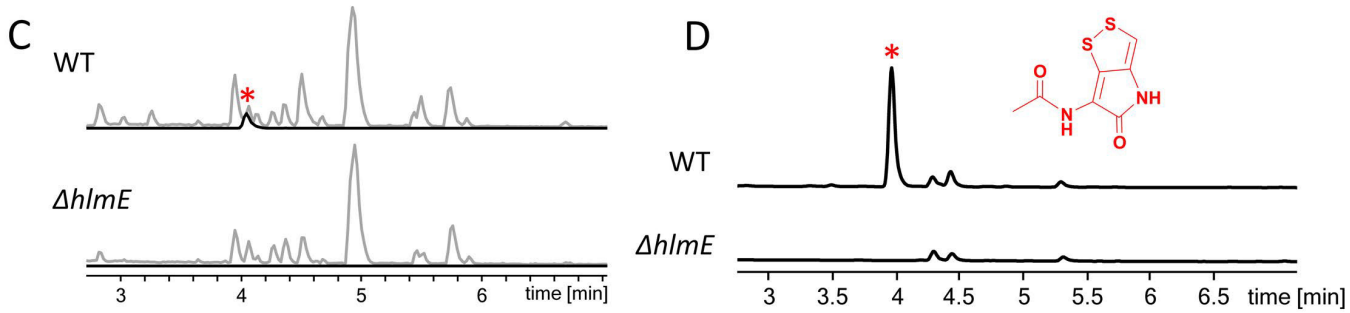

MS data, extracted ion chromatograms

UV-VIS data on wavelength 390 ± 10 nm

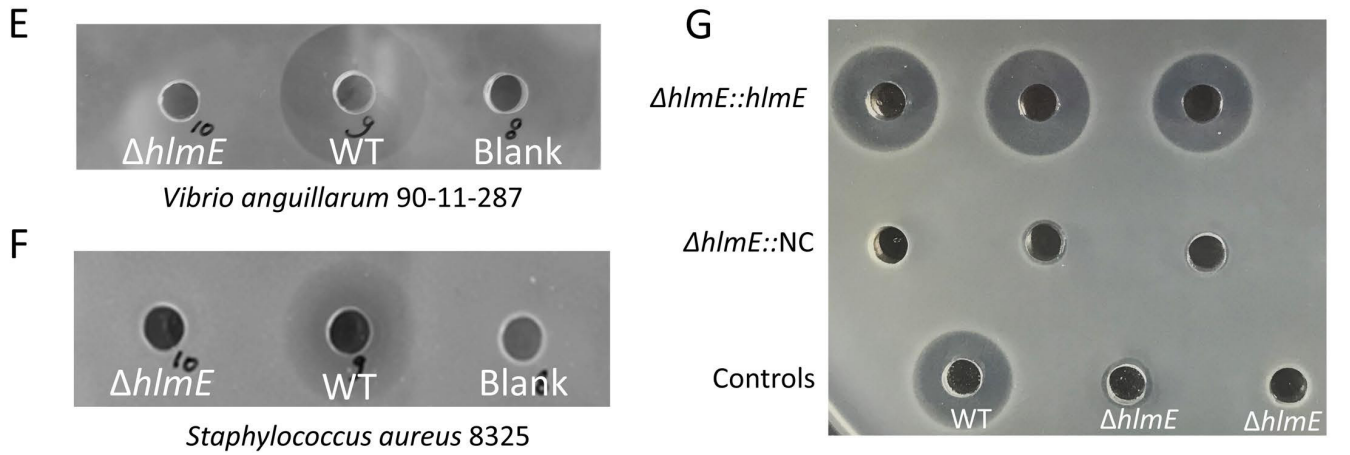

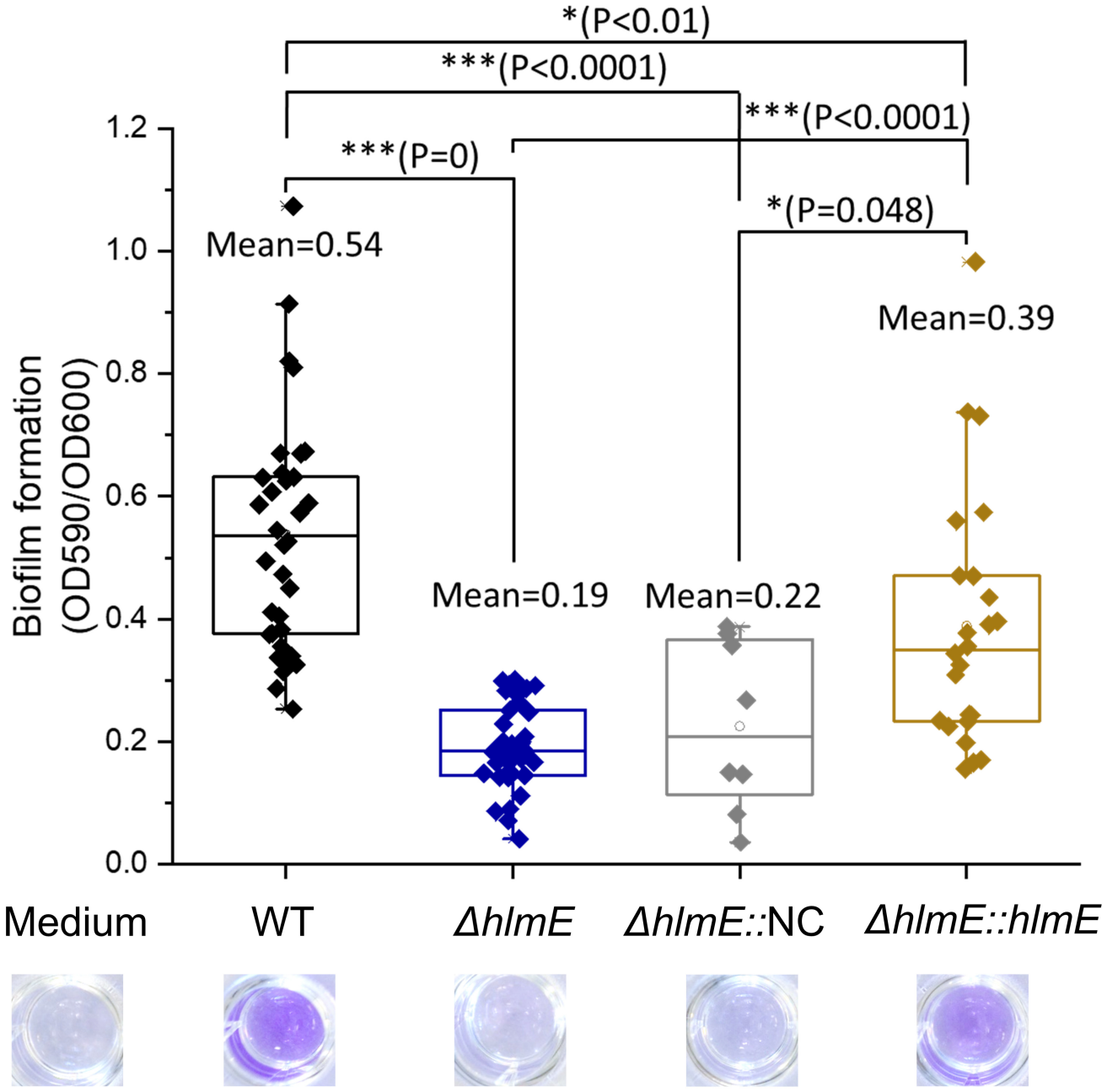

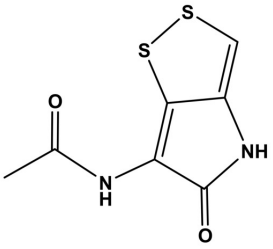

(**1**) Holomycin

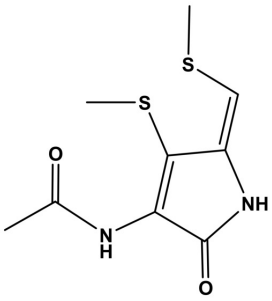

(**2**) S,S'-dimethyl holomycin